

Skull Flexure as a Contributing Factor in the Mechanism of Injury in the Rat when Exposed to a Shock Wave

RICHARD BOLANDER,¹ BLAKE MATHIE,¹ CYNTHIA BIR,¹ DAVID RITZEL,² and PAMELA VANDEVORD^{1,3}

¹Department of Biomedical Engineering, Wayne State University, 818 W Hancock, Detroit, MI 48201, USA;

²Dyn-FX Consulting Ltd., 19 Laird Ave N, Amherstburg, ON N9V 2T5, Canada;

and ³John D Dingell VAMC, Detroit, MI 48201, USA

(Received 6 April 2011; accepted 23 June 2011; published online 7 July 2011)

Associate Editor Stefan M Duma oversaw the review of this article.

Abstract—The manner in which energy from an explosion is transmitted into the brain is currently a highly debated topic within the blast injury community. This study was conducted to investigate the injury biomechanics causing blast-related neurotrauma in the rat. Biomechanical responses of the rat head under shock wave loading were measured using strain gauges on the skull surface and a fiber optic pressure sensor placed within the cortex. MicroCT imaging techniques were applied to quantify skull bone thickness. The strain gauge results indicated that the response of the rat skull is dependent on the intensity of the incident shock wave; greater intensity shock waves cause greater deflections of the skull. The intracranial pressure (ICP) sensors indicated that the peak pressure developed within the brain was greater than the peak side-on external pressure and correlated with surface strain. The bone plates between the lambda, bregma, and midline sutures are probable regions for the greatest flexure to occur. The data provides evidence that skull flexure is a likely candidate for the development of ICP gradients within the rat brain. This dependency of transmitted stress on particular skull dynamics for a given species should be considered by those investigating blast-related neurotrauma using animal models.

Keywords—Blast, Injury, Mechanism, Explosion.

INTRODUCTION

Due to the current military campaigns and social unrest around the world, the exposure of humans to explosions continues to take place.^{10,11,15} A classification system has been invented to describe the manner in which a specific pathology will develop as a result of the trauma caused by the explosion.^{12,13,16} The manner

in which the shock wave from the explosion causes trauma (primary blast injury) remains a major concern to researchers investigating this injury pattern because of its ambiguous nature.¹⁹

Multiple hypotheses describing how this injury may result have been suggested. Courtney and Courtney⁷ have recently summarized the major hypotheses of the mechanism of primary blast injury. One hypothesis is that the blast wave will compress the thorax and a resulting pressure surge to the head will cause brain injury.^{1,3} This hypothesis has been discussed as early as 1916.¹⁸ A second injury mechanism that is hypothesized states that a combination of rotational and translational accelerations resulting from shock wave interaction with the head will be great enough to cause injury.^{8,21}

A third hypothesis provided by Courtney and Courtney⁷ involves the transmission of the blast energy directly through the cranium. However, the physics of direct stresswave transmission should be distinguished from waves imparted by skull flexure. Direct wave transmission (trans-osteal wave propagation) in this case concerns the processes by which an air-borne shock wave interacts with the material interface of the skull and transmits a ‘through-thickness’ stress by direct compression of the skull material. The deformations caused by this mode of energy transfer will result in high frequency, low amplitude perturbations, similar to acoustic transmission. The development of the reflected pressure on the skull surface can also transmit enough energy to cause skull flexure. This deformation, in turn, may also cause changes in the pressure environment within the brain. Computer models have observed this transmission of blast energy in humans, but have yet to validate the results against experimental data.^{4,17,22}

Courtney and Courtney⁷ reference the work from Chavko *et al.*⁵ which reports that ICP records within the cranium are very similar in pressure to the external

Address correspondence to Pamela VandeVord, Department of Biomedical Engineering, Wayne State University, 818 W Hancock, Detroit, MI 48201, USA. Electronic mail: dt8583@wayne.edu, blakemathie@gmail.com, cbir@wayne.edu, dritz@dyn-fx.com, pvord@wayne.edu

static pressure condition. However, Leonardi *et al.*¹⁴ compared records from unsealed and completely sealed intracranial pressure (ICP) sensors from rodents exposed to a shock wave which indicated that the observation by Chavko may have been an artifact of an unsealed ICP gauge. The study by Leonardi *et al.* indicated that by creating a fully sealed testing environment, mimicking the actual physiological environment, peak ICP profiles exceeding the external static pressure environment will develop. The unsealed environment produced similar recordings to those of the external pressure measurements since the enhanced fluid pressurization was able to be relieved through the leaking seal. They also noted distinct ICP oscillations taking place in the signal following the initial pressure rise, the amplitude, and frequency of the imparted ICP was likely linked to skull dynamics.

Other researchers have also observed an oscillatory ICP response following an initial rise in pressure, with the response depending on the dampening of the tissues tested.^{6,20} In order to determine the source of ICP oscillations, Romba and Martin²⁰ investigated the effect of shielding the thorax of the Rhesus monkey while subjecting the head to blast exposure. Their results indicated that ICP oscillations were found regardless of the presence of thorax protection. Recently, similar results demonstrated that strong blast-induced ICP was inflicted in swine despite being fitted with thoracic protection.² A pressure pulse was generated in the inferior vena cava during exposure, but the delay was approximately two ms with a much longer rise time to peak pressure. Additionally there was no parallel increase in the ICP profiles relative to this pulse.

In the case of head exposures to shock waves, it is hypothesized that the dynamic structural response modes of the skull, with the associated viscoelastic brain mass acting as a coupled mechanical system, controls the stress (pressure) imparted to brain tissue under shock wave loading. The dynamic response modes of the skull, and hence imparted ICP, will relate to its particular geometry and material characteristics.

An experiment was designed to confirm this hypothesis will provide valuable information to identify particular modes of the coupled skull/brain response and their correlation with the ICP waveforms developed. Components of the imparted high strain rates in the form of ICP profiles may contribute to the cellular injury reported after blast exposure. The goal of this study was to examine and identify the critical biomechanical contributions of the shock wave interactions using a rodent model of blast neurotrauma. Independent methods for measuring skull strain and ICP were applied. Subsequent analysis of the rodent skull was used to further characterize potential areas of

skull flexure. Currently information regarding the response of the rat head to shock wave exposure is lacking in the literature and this series of experiments will provide much needed insights into the underlying biomechanics of blast neurotrauma.

METHODS

Wayne State University (WSU) Shock Wave Generator

The WSU shock wave generator is a shock tube system that is based on a commonly employed system for the generation of well formed, controlled shock waves.⁹ The system has a driver section that is separated from the driven chamber by a frangible membrane and is pressurized with compressed helium. Upon membrane rupture, the rapid expansion of gas in the tube drives an air shock wave into the test section. The event is measured by pressure sensors (Model 102A06, PCB Piezotronics Inc.) at positions along the length of the shock tube. Shock wave amplitude is controlled by varying the thickness of the frangible membrane. As the thickness of the membrane increases, the pressure within the driver will increase prior to rupture of the diaphragm. The increased pressure during rupture of the diaphragm will generate greater shock wave amplitudes. Specific details of the WSU shock wave generator are documented in Leonardi *et al.*¹⁴

Animal Testing

Approval of all experiments was obtained from the Wayne State University Institutional Animal Care and Use Committee (IACUC) prior to testing. A total of ten male Sprague–Dawley rats, age 65–70 days old, were procured. All animals were given food and water *ad lib*. Animals were randomly assigned to one of two groups based on instrumentation used during the testing: strain gauge (SG) or ICP sensor mounted to the top of the skull (IC).

Animal Preparation and Sensor Installation for SG Testing

Five SG rats were sacrificed immediately prior to testing. The dermal tissue was removed from the medial dorsal surface of the head exposing a 1.5 cm wide region of the skull extending from 1 cm rostral to the bregma to 1 cm caudal to the lambda. The skull surface was then cleaned using acetone to ensure a solid and durable mechanical bond with the strain gauge. A 3-axis rectangular Rosette-style strain gauge (FAER-25B-35SX, Vishay Micro-measurements Inc.) was then attached to the skull surface using

cyanoacrylate and allowed five minutes to cure. To limit motion of the rat's head during exposure and prevent mechanical stress on the instrumentation wires, the nose was secured such that the head was pitched down at approximately 45° to the shock front. The channels were named rostral, medial, and caudal (Fig. 1a).

Animal Preparation and Sensor Installation for IC

Five IC designated rats were anesthetized using a ketamine/xylazine mixture (80 mg/kg/10 mg/kg; I.P.) and immobilized in a stereotaxic frame. A longitudinal incision was made along the dorsal medial surface of the head, exposing the skull from the bregma to the lambda. A 1.5 mm diameter hole was drilled using a stereotaxic high-speed drill at the following location: +3.0 (A-P (mm) from Bregma), -2.0 (M-L (mm)), and -1.0 (D-V (mm)), exposing the frontal cortex.

A plastic guide cannula (18 gauge; 1.2 mm, CMA Microdialysis Inc.) with a small pedestal was implanted through the hole and fixed to the skull using two small stainless steel screws inserted at 45° angles from the horizontal into the skull adjacent to the cannula. Cranioplastic cement was applied to fix the pedestal to the skull and was anchored by the screws. The surgical wound was closed with sutures, as needed. A dummy cannula insert with a threaded cap was inserted in the guide cannula until shock exposure; the rats were allowed five days recovery time.

Prior to testing, rats were anesthetized using a ketamine/xylazine mixture (80 mg/kg/10 mg/kg; I.P.). The cannula was then filled with a sterile saline solution. The cannula cap was filled with petroleum jelly and the fiber optic pressure sensor (FOP-MIV, Fiso Inc.) was inserted into the cannula and threaded onto the cannula pedestal. Figure 1b provides a sketch of the technique applied.

Shock Wave Exposure

The rat was affixed to a trolley-mounted stage using a nylon harness, and inserted into the shock tube, such that its nose was positioned 114 cm inside the end of the Lexan® tube opposite to, and facing, the driver (Fig. 2). The harness maintained the rat's longitudinal axis perpendicular to the shock front and in fixed proximity to a side-on pressure sensor. The trolley system reduced the effects of post-shock dynamic pressure flow on the rat.

Once placed in the harness, the SG rats were subjected to three exposures each at 69, 97, 117, and 172 kPa static shock pressure or until sensor failure, thus a total of 12 exposures per animal. The IC rats were exposed to three repeated exposures at three intensities (69, 97, and 117 kPa). In order to conserve the integrity of the ICP sensors, the highest pressure

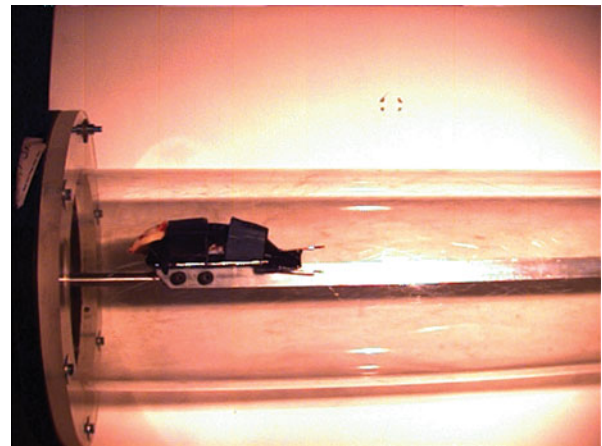


FIGURE 2. The rat was placed 114 cm within the shock tube and was placed on a trolley system to reduce the level of dynamic pressure shifts that are not representative of a free field shock wave.

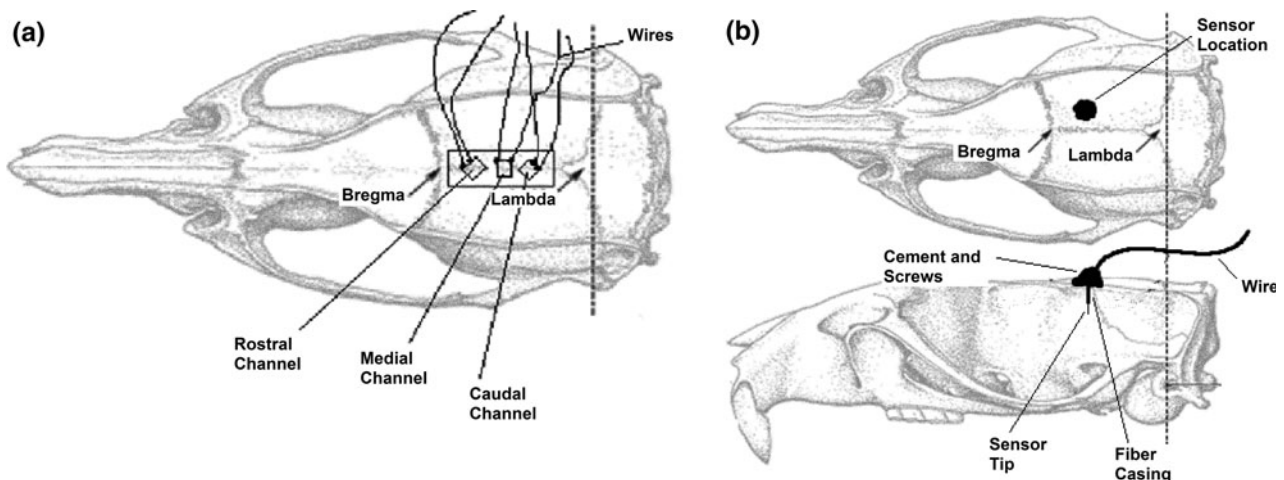


FIGURE 1. Placement of strain gauge on surface of the rat skull (a). Fiber optic pressure sensor installation on a rat skull (b).

intensity (172 kPa) was not applied. The intensities used in the protocol were determined from previous tests to maximize the amount of useful data. The time in between exposures was approximately two minutes for both groups of animals.

Both ICP and strain data were collected at 400 kHz using the Dash 8HF data acquisition system (Astro-med Inc.). The data was then post-processed completely using Diadem 11.0 (National Instruments Inc.). Calculations of maximum principal strain were made using the formula below; the rostral channel was measured as ε_1 , the medial channel was measured as ε_2 , and the caudal channel was measured as ε_3 .

$$\varepsilon_{P,Q} = \frac{\varepsilon_1 + \varepsilon_3}{2} \pm \sqrt{\left[(\varepsilon_1 - \varepsilon_2)^2 + (\varepsilon_2 - \varepsilon_3)^2 \right] / 2}$$

The data was then reported in microstrain, and the magnitude of the first compressive peak was recorded. The IC pressure data was also analyzed, including peak pressure and rate of pressure change. Data was grouped by shock wave intensity and responses were compared using ANOVA with *post hoc* Tukey HSD used to determine significant differences ($p < 0.05$) between groups.

Computer Tomography (CT) Imaging

Following the experimental test series, computed tomography (CT) scans were obtained for the SG rats by means of a microCT device (Scanco VivaCT, Scanco Medical Inc.). ICP rats were not scanned as the instrumentation installed into the skull made it difficult to measure bone thickness. Variability of SG rat skull thickness throughout the skull was determined to help identify structural weaknesses that could be considered candidates for flexure. Skulls were scanned using a voltage of 70 kVp and current of 114 μ A at a 30 μ m resolution with a 320 ms integration time. Thickness measurements were calculated by using microCT analysis software (Scanco Medical Inc.). Measurements were taken at the midpoint between the lambda and bregma sutures. Three-dimensional reconstruction of the skull was undertaken to appreciate the skull geometry.

RESULTS

SG Measurements

The data collected from the strain gauges was useful for determining the flexural response of the superior braincase to shock wave loading. There were characteristic superimposed response patterns that were observed consistently as follows: (1) A strong and rapid compression with an associated damped oscillation at relatively high frequency (less than 3 kHz). (2)

A quasi-steady decompression closely following the decay of the external static overpressure condition that developed as the strain returned to pre-blast levels. (3) A waveform of lower frequency with its pulse beginning in tension following the rapid compression. These responses were present for all the rats tested and are shown in Fig. 3.

The waveforms from two different rats are presented in Fig. 3, and the characteristic responses described prior are observable for both series. The first trace in each series is from the side-on (static) pressure sensor exposed to the incident shock wave. Within both series, following the incident shock, reflections from the fixture holding the specimen develop and create pressure artifacts on the sensor's surface that are not representative of the environment to which the specimen is exposed. This effect is expected from theory; the arrival and amplitude of the perturbation coincides with those expected of that reflection disturbance; confirmation of this phenomenon is also demonstrated by the fact that the shock reflections are similar between series, while the strain response is specific to the specimen being tested.

The peak compression was reported for all exposures. In Fig. 4a, it is shown that as the incident shock wave intensity increased, the calculated maximum principal strain also increased. The means were significantly different between groups ($*p < 0.05$).

ICP Measurements

For the ICP profiles, two response patterns were observed consistently between specimens. (1) The peak compression wave will rebound and oscillate in a dampened harmonic motion. (2) There was a rapid increase in pressure that approximates the external loading environment and then returns to pre-exposure conditions. In Fig. 4b, 4c it is shown that as the incident shock wave intensity increased, the peak pressure and maximum rate of pressure change both increased.

The pressure response profiles for a 249 gm rat are shown in Fig. 5. The three profiles have been time shifted to begin at the same point. The increase in peak pressure as a function of an increase in incident side-on pressure can be observed for this series of wave forms. The duration of the rise times is also a function of intensity, where the greatest intensities resulted in the shortest rise times. To further this point, the 97 kPa ICP wave form was time shifted so that its pressure profile could be compared to a 97 kPa incident shock wave without the shock reflections that were observed in Fig. 5 (Fig. 6). The rise times between the incident wave as measured by the side-on pressure sensor and the ICP wave is of interest (27 compared to 195 μ s). Although the rise time of the shock front is

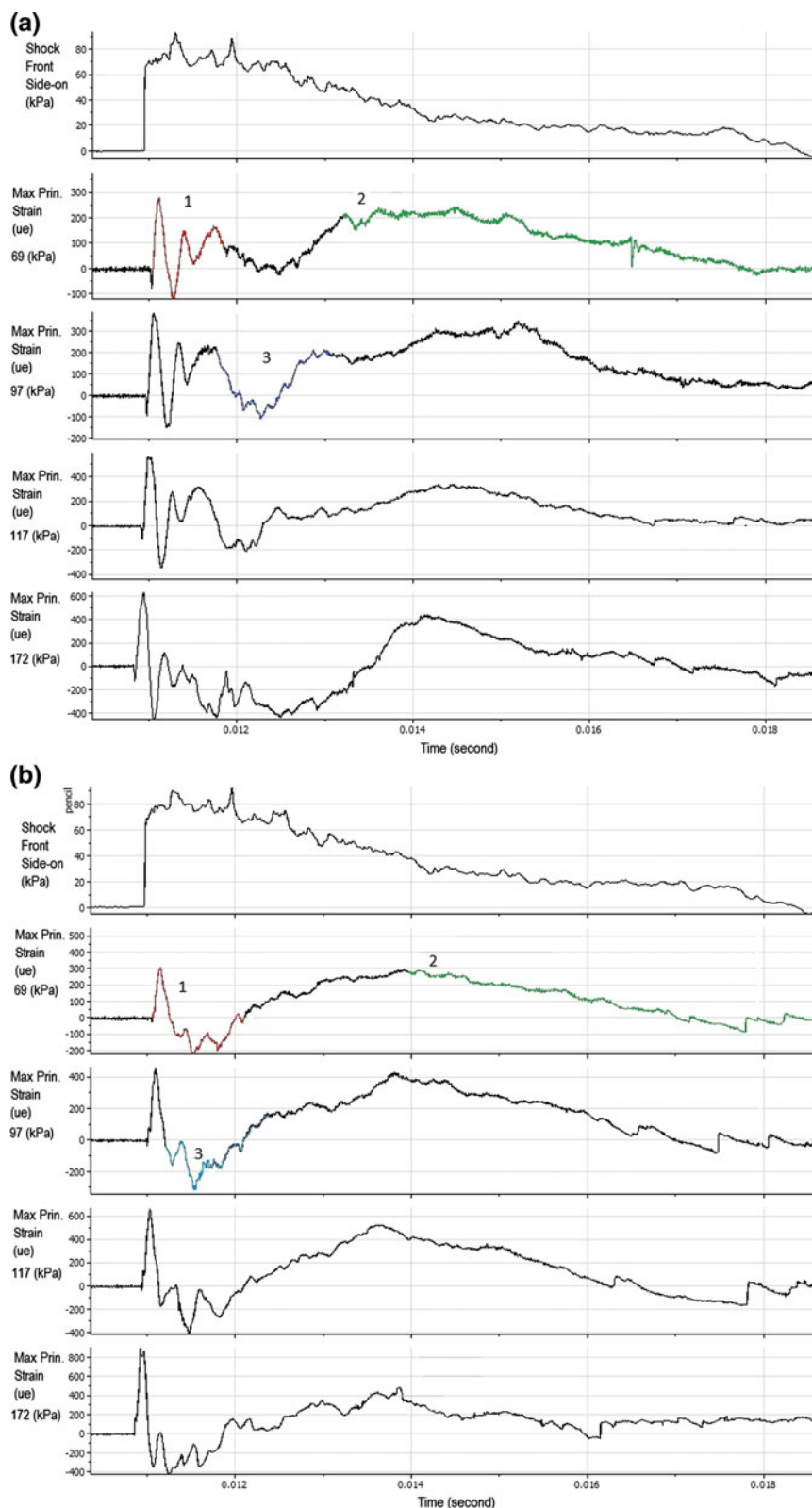


FIGURE 3. The principal strain response profiles of the superior brain case for both a 262 and 247 gm rat when exposed to shock waves of increasing intensity. The magnitude for each profile is adjusted so that the frequency content is observable. For the presented data, tension is negative and compression is positive. (1) A strong and rapid compression with an associated damped oscillation at relatively high frequency (less than 3 kHz). (2) A quasi-steady decompression closely following the decay of the external static overpressure condition that developed as the strain returned to pre-blast levels. (3) A waveform of lower frequency with its pulse beginning in tension following the rapid compression.

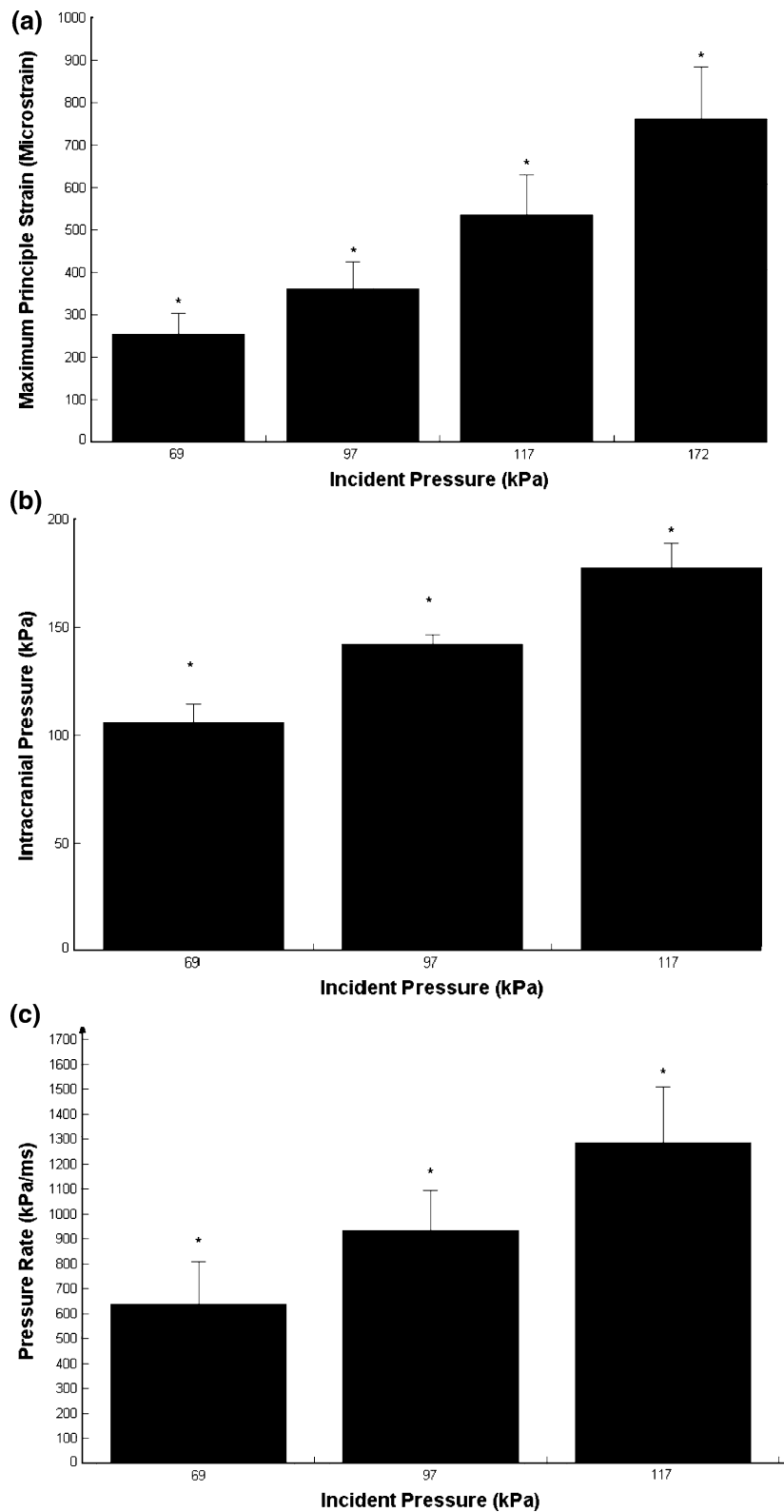


FIGURE 4. (a) The initial compression of the skull is dependent on intensity of the incoming shock wave. The largest magnitude shock waves caused the greatest maximum principal strains. All groups were significantly different from each other ($*p < 0.05$). (b) The ICP will increase beyond that of the incident shock wave ($*p < 0.05$). (c) The rate of pressure change will also increase with intensity ($*p < 0.05$).

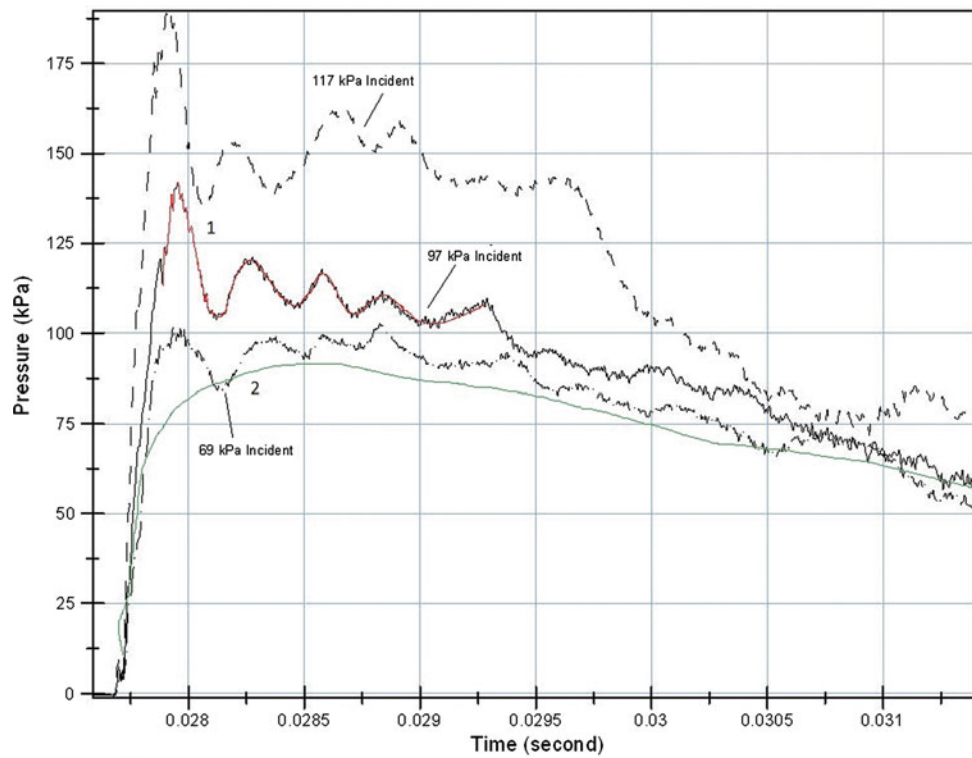


FIGURE 5. The intracranial pressure response of a rat skull is dependent on shock wave intensity. The ICP responses for a 249 gm rat show distinct pressure fluctuations (1) (red) that are present in each of the profiles that last for less than 2 ms. The waveforms will also approximate the external loading response invoked by the shock wave (2) (green).

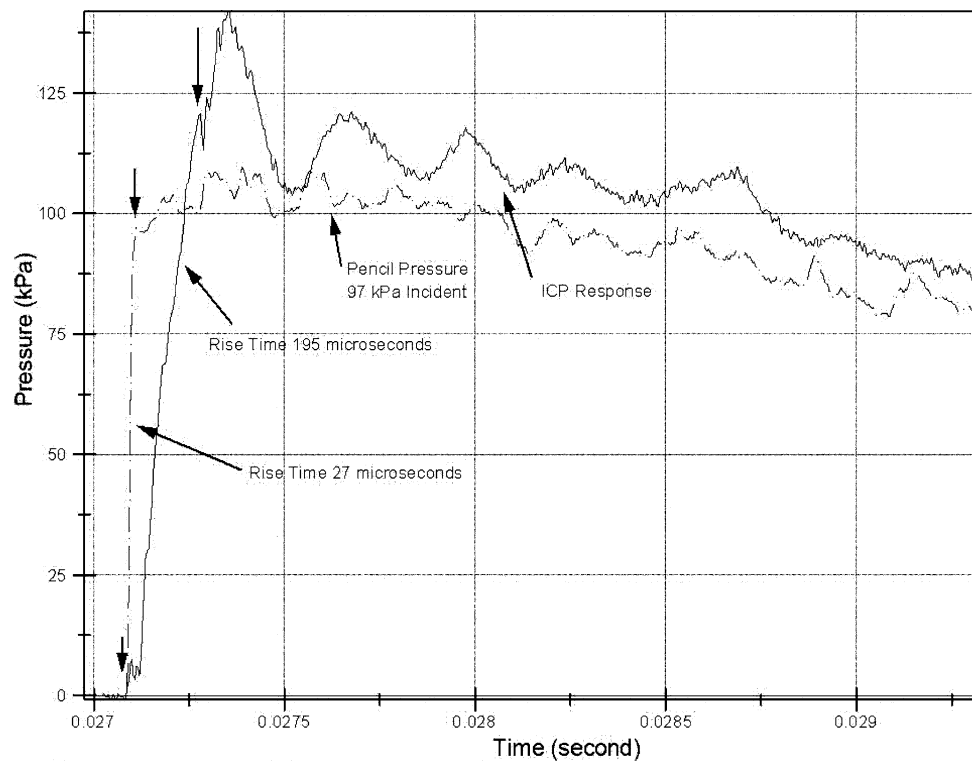


FIGURE 6. The rise time of the external pressure wave is faster than the rise time of the record intracranial pressure for a 249 gm rat. It is hypothesized that this is due to the amount of energy that is required to deform the skull so that a pressure wave can develop within the brain.

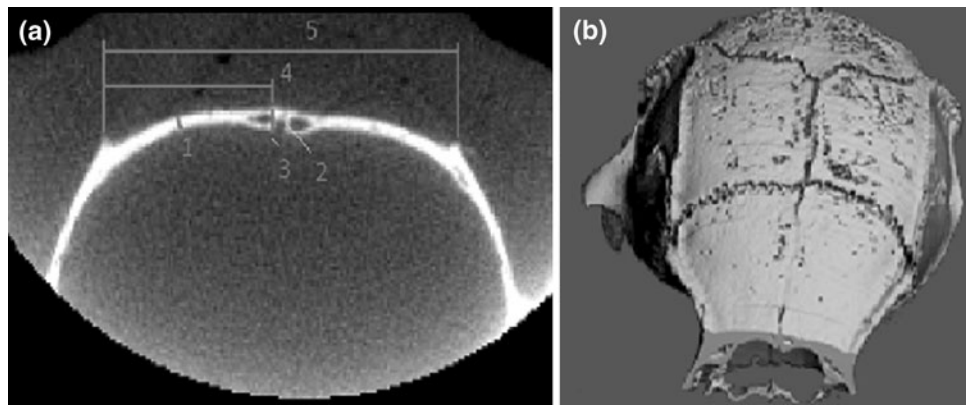


FIGURE 7. (a) Measurements were taken of the MicroCT images of the rat skull to determine key structural elements. (b) A three-dimensional reconstruction of the images depict that there are considerable gaps between the bone plates with significant reinforcement on the lateral bone folds, suggesting that the midline suture will be a probable place for skull flexure to take place.

approximately $1 \mu\text{s}$ the $27 \mu\text{s}$ measured is an artifact that is created by displacing the sensing element. It is expected that this delay between the two pressure profiles is caused by the absorption of energy that takes place by causing the skull to flex, thereby increasing ICP.

MicroCT Imaging

The results from the microCT imaging provided information regarding the geometry and thickness of specific bones in the skull (Fig. 7a). The mid-plate thickness between lambda and bregma sutures was approximately 0.354 ± 0.061 mm thick (1) where the thickness increases near the midline suture to 0.630 ± 0.082 mm thick (3). The gap between the suture itself was approximately 0.162 ± 0.016 mm thick (2). At this point the distance from horn to horn was 11.72 ± 0.114 mm (5). Additionally the distance from horn to suture top was 5.78 ± 0.207 (4). A sample of measurement locations are indicated in Fig. 7a. The image is of a cross section of head mid-distance between the lambda and bregma sutures. The term horn is in reference to the folds of bone on the lateral aspects of the skull, acting as reinforcements. Values are reported as (mean \pm SD).

In Fig. 7b a three-dimensional reconstruction of the rat skull is provided. The rostral end was rotated down to the bottom of the graphic; the caudal region is near the top. The locations of the suture lines indicate that inward flexure of the superior bones of the skull case is probable during exposure due to the static pressure as it traverses the head.

DISCUSSION

Recent experimental biomechanical data for the rat suggested that skull flexure contributes to the ICP

gradients developed within the brain as a result of shock wave interaction.¹⁴ Results from the current experiments validate the hypothesis by Leonardi *et al.*¹⁴ demonstrating that strain on the skull surface may have a significant effect on the imparted ICP waveform. By applying a series of pressure intensity exposures, it was observed in this study that the ICP response was dependent on the incident shockwave intensity. Further, the rate of pressure change was found to increase while the rise time to peak pressure was found to decrease with intensity.

When the ICP response was compared to the pressure profile of the incident shock wave, a delay in the rise time of the ICP was observed. This suggests that the rat skull is acting as a medium between the external environment and the intracranial contents. Pressure recordings reported by Bauman *et al.*² also found a significant delay in the rise time of the ICP profile compared to the incident shock wave during their swine testing. It is hypothesized that the rise time of those ICP profiles within the swine will be longer than that of the rat because of the difference in skull thickness between species. More studies need to be conducted to verify this relationship.

The microCT imaging of the superior braincase of the rat revealed that the bones are not completely fused and the lateral aspects are reinforced with thicker layers of bone. It is hypothesized that when the incident shock wave traverses the surface of the skull, the shock wave is acting as a moving load. This loading will cause the greatest deflections in the regions with the least reinforcement. When examining the specific anatomical features of the rat skull, the region between the lambda and bregma suture appears to offer the greatest amount of deflection as the bone plates may hinge about the major sutures.

The results from the strain gauge data further substantiates the hypothesis that the incident shock wave

is causing the skull to flex. The rapid compression that increases in magnitude with the intensity of the incident shock is believed to be the direct result of the shock wave compressing the skull surface. The damped harmonic oscillation phase that then developed as a result of the compression is hypothesized to be due to the return of the deflected surface regions back to equilibrium. The quasi-steady decompression phase that approximates the external pressure environment is then best observed due to the dispersion of the energy from the rapid compression of the skull case. The nature of the secondary surface wave beginning in tension has yet to be determined. It has been observed that this wave is dependent on the intensity of the incident shock wave. The front of this wave will be steeper as the intensity increases. Research is ongoing to determine the nature of this wave.

Because of these observations in both the strain gauge and ICP responses, it is proposed that there are two major regions in the waveform response. The first is the transient phase which consists of a rapid compression and harmonic oscillations; the other is the quasi-steady decompression phase. It is possible that the most damaging aspect of these waveforms is the initial oscillations that may cause high levels of strain rates in both tension and compression that could be transferred as rapid compression waves within the brain due to the coupling at the skull/dura interface.

Some limitations exist with the current data. The placement of the strain gauge on the skull is problematic because mounting on the suture lines will cause an amplification of the signal. Although the results provided key information, the principal strain calculations were not made on a homogenous surface and the sensors were relatively widely distributed. But, given the consistency of the signals between exposures and that similar responses were observed between species, the data is useful for describing responses of the rat skull to shock wave exposure.

The ICP data was of concern because the skull was modified with small screws and bone cement, modifying the native surface. If the superior skull case is acting as a diaphragm, the additional mass of the sensor cement complex will cause the periodic oscillations to have a response with fewer competing frequencies than what are observed in the strain profiles. This can be seen in Fig. 5, specifically for the 97 kPa incident exposure. Additionally, it still needs to be determined to what extent the fiber optic sensors are mapping the motion of the skull when compared to the environment within the brain. Because of the artifacts of testing with the ICP sensors, direct relationships were not made to the strain gauges. Further studies are required to address this issue.

It is expected that the biomechanical responses of the rat will be unique when compared to other species. It would be ideal to be able to equate injury responses in rats to humans, but scaling for thresholds of injury cannot be conducted until the mechanism of injury is discovered. The human head is much more spherical and thicker in geometry as compared to the rat. These changes may result in different response modes than what are observed in the rat. Because the mechanical inputs into the brain are likely specific to the system, a multi species analysis of skull flexure and ICP will need to be undertaken.

In summary, this article provides key biomechanical data which suggests that skull flexure may be one of the major factors for causing ICP gradients. The superior rat skull is a location where flexure will be exaggerated. Since neuronal injury is dependent on strain rate, it is hypothesized that the first two ms following exposure (the transient phase) is the likely timeframe for causing neurotrauma. This period is composed of extremely rapid shifts in strain that are likely transmitted to the cells within the brain. It is not yet known which aspects of the intracranial pressure profile causes cellular injury. Ultimately, it is of utmost importance to evaluate cellular vulnerability under the particular stress-rate conditions observed. Utilizing appropriate *in vitro* experiments for blast-related neurotrauma will help identify biomarkers of neuropathology and shifts in gene expression occurring as a result of shock wave exposure.

ACKNOWLEDGMENTS

We would like to thank the WSU Bioengineering Center staff and students for assisting with this project. We would also like thank Dr. Amanda Esquivel for obtaining the CT images. This project was partially funded by DOD Award Number W81XWH-08-2-0207 and the Thomas J. Rumble Fellowship.

REFERENCES

- ¹Battacherjee, Y. Shell shock revisited: solving the puzzle of blast trauma. *Science* 319:406–408, 2008.
- ²Bauman, R., G. Ling, L. Tong, A. Januszkievicz, D. Agoston, N. Delanerolle, J. Kim, D. Ritzel, R. Bell, J. Ecklund, R. Armonda, F. Bandak, and S. Parks. An introductory characterization of combat casualty care relevant swine model of closed head injury resulting from exposure to explosive blast. *J. Neurotrauma* 26:841–876, 2009.
- ³Cernak, I. Penetrating and blast injury. *Restor. Neurol. Neurosci.* 23:139–143, 2005.

- ⁴Chafi, M., G. Karami, and M. Ziejewski. Biomechanical assessment of brain dynamic responses due to blast pressure waves. *Ann. Biomed. Eng.* 38:490–504, 2010.
- ⁵Chavko, M., W. Koller, W. Prusaczyk, and R. McCarron. Measurement of blast wave by a miniature fiber optic pressure transducer in the rat brain. *J. Neurosci. Methods* 159:277–281, 2007.
- ⁶Clemedson, C., and C. Criborn. Mechanical response of different parts of a living body to a high explosive shock wave impact. *Am. J. Physiol.* 181:471–476, 1955.
- ⁷Courtney, M., and A. Courtney. Working toward exposure thresholds for blast-induced traumatic brain injury: thoracic and acceleration mechanisms. *Neuroimage* 54:S55–S61, 2011.
- ⁸Finkel, M. The neurological consequences of explosives. *J. Neurol. Sci.* 249:63–67, 2006.
- ⁹Henshall, B. Shock tube—versatile tool of aerodynamic research. *J. Royal Aeronaut. Soc.* 58:541–546, 1954.
- ¹⁰Hicks, R., S. Fertig, R. Desrocher, W. Koroshetz, and J. Pancrazio. Neurological effects of blast injury. *J. Trauma* 68:1257–1263, 2010.
- ¹¹Hoge, C., D. McGurk, J. Thomas, A. Cox, C. Engel, and C. Castro. Mild traumatic brain injury in U.S. Soldiers returning from Iraq. *N. Engl. J. Med.* 358:453–463, 2008.
- ¹²Kluger, Y., A. Nimrod, P. Biderman, A. Mayo, and P. Sorkin. The quinary pattern of blast injury. *Am. J. Disaster Med.* 2:21–25, 2007.
- ¹³Lechner, R., G. Achatz, T. Hauer, H. Palm, A. Lieber, and C. Willy. Patterns and causes of injuries in a contemporary combat environment. *Unfallchirurg* 113:106–113, 2010.
- ¹⁴Leonardi, A., C. Bir, D. Ritzel, and P. VandeVord. Intracranial pressure increases during exposure to a shock wave. *J. Neurotrauma* 28:85–94, 2011.
- ¹⁵Ling, G., and J. Ecklund. Traumatic brain injury in modern war. *Curr. Opin. Anaesthesiol.* 24:124–130, 2011.
- ¹⁶Luks, F. Blast injuries—and the pivotal role of trauma surgeons. *Acta Chir. Belg.* 110:517–520, 2010.
- ¹⁷Moss, W., M. King, and E. Blackman. Skull flexure from blast waves: a mechanism for brain injury with implications for helmet design. *Phys. Rev. Lett.* 103:108702, 2009.
- ¹⁸Mott, F. On the effects of high explosives upon the central nervous system. *Lancet* 187:331–338, 1916.
- ¹⁹Risling, M. Blast induced brain injuries—a grand challenge in TBI research. *Front. Neurol.* 8:1, 2010.
- ²⁰Romba, J., and P. Martin. The propagation of air shock waves on a biophysical model. US Army Ordinance Technical Memorandum, pp. 17–61, 1961.
- ²¹Stuhmiller, J., K. Ho, M. VanderVorst, K. Dodd, T. Fitzpatrick, and M. Mayorga. A model of blast overpressure injury to the lung. *J. Biomech.* 29:227–234, 1996.
- ²²Taylor, P., and C. Ford. Simulation of blast-induced early time intracranial wave physics leading to traumatic brain injury. *J. Biomech. Eng.* 131:061007, 2009.